arXiv:1609.07229v1 [math.OC] 23 Sep 2016

# Optimal Power Consumption for Demand Response of Thermostatically Controlled Loads

Abhishek Halder*, Xinbo Geng*, Fernando A.C.C. Fontes†, P.R. Kumar*, and Le Xie*

***Abstract*— We consider the problem of determining the optimal aggregate power consumption of a population of thermostatically controlled loads. This is motivated by the problem of synthesizing the demand response for a load serving entity (LSE) serving a population of such customers. We show how the LSE can opportunistically design the aggregate reference consumption to minimize its energy procurement cost, given day-ahead price, load and ambient temperature forecasts, while respecting each individual load's comfort range constraints. The resulting synthesis problem is shown to be amenable to optimal control techniques, but computationally difficult otherwise. Numerical simulations elucidate how the LSE can use the optimal aggregate power consumption trajectory thus computed, for the purpose of demand response.**

## I. Introduction

Motivated by the goal of sustainable electricity generation, renewables such as solar and wind are of increasing interest as electric energy resources. Concomitantly, the inherent time variability of such renewable generation is in turn shifting modern power system operation from the traditional "supply follows demand" paradigm to the one where "demand adapts to supply". This new operational paradigm, called "demand response" [1], [2], can leverage demand side flexibility to offset variability in generation. Of particular interest in this context are thermostatically controlled loads (TCLs) such as air conditioners. In this paper we examine how an "aggregator" also known as a "load serving entity" (LSE), can employ a population of its customers' TCLs to shape the aggregate power consumption, while adhering to each load's comfort constraints. We consider an LSE buying energy from the day-ahead market for a population of TCLs. We address the question of designing the optimal aggregate power consumption trajectory for this population, given a forecast of day-ahead price trajectory.

### A. Related Work

Modeling the dynamics of a population of TCLs has been investigated in several papers [3]–[10], with the aim to derive control-oriented models that can accurately predict the aggregate power trajectory. Once such a model is obtained, the predominant focus in these and other papers [11]–[13] is to design a model-based setpoint controller to enable the TCL population track a given reference aggregate power trajectory in real-time, thereby compensating possible mismatch between the real-time and forecasted ambient temperatures. Although the availability of a reference power trajectory is tacitly assumed in the literature, in practice the LSE needs to determine this reference to minimize the energy procurement cost while guaranteeing that the reference trajectory can be tracked by the aggregate dynamics in such a manner that individual comfort range constraints are met. In [14], the range of feasible reference power trajectories is studied. To the best of the authors' knowledge, the present paper is first to focus on determining the optimal reference power consumption while respecting end users' comfort zones.

### B. Contributions of This Paper

Assuming that the LSE is managing a finite population of TCLs, we formulate and solve the optimal aggregate power consumption design as a finite horizon deterministic optimal control problem. In the presence of state inequality constraints arising from comfort range contracts between the LSE and individual TCLs, the optimal controls are shown to depend on the minimum chattering amplitude at the upper and lower comfort boundaries allowable by the thermostat. Our results provide analytical insights on how the LSE can use the knowledge of day-ahead price forecast, load forecast, and ambient temperature forecast, for the purpose of energy procurement at least cost.

This paper is organized as follows. In Section II, we describe the mathematical models. In Section III, we formulate the design of power consumption as an optimal control problem. Sections IV and V present the solution of the power consumption design problem. In Section VI, numerical results based on the day-head price forecast data from Electric Reliability Council of Texas (ERCOT) and the ambient temperature forecast data from a weather station in Houston, Texas are reported, to illustrate how the LSE can use the optimal power consumption trajectory computed via the proposed framework, for the purpose of demand response. Section VII concludes the paper.

### C. Notation

We use the symbols $\mathbb{1}_X$ and $|X|$ to respectively denote the indicator function, and the Lebesgue measure of set $X$. We use $\mathbb{D}(Y)$ to denote the space of càdlàg functions whose range is set $Y$. For $a, b \in \mathbb{R}$, we use the notations $a \vee b := \max(a, b)$, $a \wedge b := \min(a, b)$, and $[a]^+ := 0 \vee a$. The symbol $\circ$ denotes the composition operator, and $\mathrm{spt}(\cdot)$ denotes the support of a function.

*Department of Electrical and Computer Engineering, Texas A&M University, College Station, TX 77843, USA, {ahalder,gengxbtamu,prk,le.xie}@tamu.edu

†ISR-Porto and Faculdade de Engenharia, Universidade do Porto, 4200-465 Porto, Portugal, faf@fe.up.pt

This material is base upon work partially supported by NSF under Contract Nos. ECCS-1546682, CPS-1239116, Science & Technology Center Grant CCF-0939370, DGE-1303378, and ECCS-1150944.

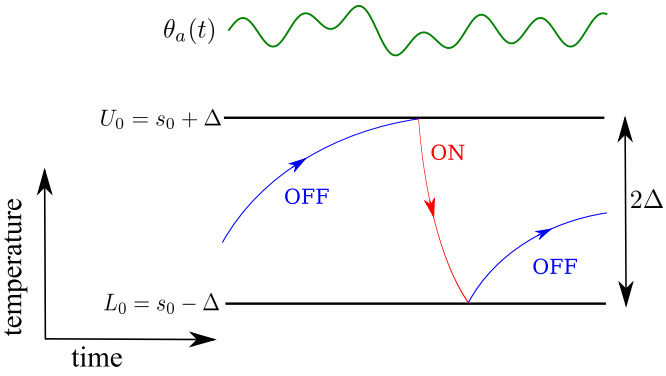


Fig. 1. The dynamic behavior of a TCL with fixed setpoint $s_0$, is illustrated for a time-varying ambient temperature $\theta_a(t)$. The comfort temperature interval for the TCL is $[L_0, U_0]$ with range $U_0 - L_0 = 2\Delta$. The indoor temperature trajectory $\theta(t) \in [L_0, U_0]$ consists of alternating OFF (*blue, up-going*) and ON (*red, down-going*) segments, with the boundaries $L_0$ and $U_0$ acting as reflecting barriers for the ON and OFF segments, respectively.

## II. Model

### A. Dynamics of Individual Thermostatically Controlled Load

The dynamic behavior of an individual TCL is shown in Fig. 1. At time $t$, let us denote the indoor temperature by $\theta(t)$, and the ambient temperature by $\theta_a(t)$. At $t = 0$, an occupant privately sets a temperature $s_0 := s(0)$, called setpoint, close to which the indoor temperature $\theta(t)$ must lie at all times. If the occupant is willing to tolerate at most $\pm\Delta$ temperature deviation from $s_0$, then we define its "temperature comfort range" as $[L_0, U_0] := [s_0 - \Delta, s_0 + \Delta]$. If the setpoint $s$ does not change with time, then $s(t) \equiv s_0$, and consequently, the comfort boundaries $L_0$ and $U_0$ remain fixed over time. For specificity we consider the problem of controlling air-conditioning rather than heating, though the theory developed in the sequel applies to both.

The rate of change of $\theta(t)$ is governed by Newton's law of heating/cooling given by the ordinary differential equation (ODE)

$$\dot{\theta}(t) = -\alpha\left(\theta(t) - \theta_a(t)\right) - \beta P \sigma(t), \tag{1}$$

where $\sigma(t)$ is the ON/OFF mode indicator variable of the air-conditioner, given by

$$\sigma(t) := \begin{cases} 1 & \text{if} \quad \theta(t) = U_0, \\ 0 & \text{if} \quad \theta(t) = L_0, \\ \sigma\left(t^-\right) & \text{otherwise.} \end{cases} \tag{2}$$

In other words, $\sigma(t) = 1(0)$ indicates that the TCL is in ON (OFF) mode. In (1), the parameters $\alpha, \beta, P > 0$ respectively denote the heating time constant, thermal conductivity, and amount of thermal power drawn by the TCL in ON mode. A parameter $\eta > 0$ called load efficiency, relates the thermal power drawn $P$, with the electrical power drawn $P_e$, via the formula $P_e = \frac{P}{\eta}$. The state of a TCL at time $t$ is the tuple $\{s(t), \theta(t), \sigma(t)\} \in \mathbb{R}^2 \times \{0, 1\}$.

As shown in Fig. 1, starting from an initial condition $(s_0, \theta_0, \sigma_0 = 0)$, the indoor temperature $\theta(t)$ rises exponentially until it hits the upper boundary $U_0$, at which time an OFF→ON mode transition occurs, and subsequently $\theta(t)$ decreases exponentially until it hits the lower boundary $L_0$, at which time an ON→OFF transition takes place, and so on. Thus, the dynamics of a TCL is hysteretic in the sense that if $\theta_0 \in [L_0, U_0]$, then $\theta(t) \in [L_0, U_0]$ for all $t > 0$. While the qualitative behavior shown in Fig. 1 is true for any $\theta_a(t) > U_0$, temporal variations of $\theta_a(t)$ engender time-varying heating/cooling rates for $\theta(t)$.

### B. Day Ahead Price Forecasts

We suppose that the LSE is exposed to a price forecast $\widehat{\pi}(t)$ and ambient temperature forecast $\widehat{\theta}_a(t)$, over a time horizon $[0, T]$. For example, if $T = 24$ hours, and the forecast is done on the previous day, then $\widehat{\pi}(t)$ is the forecasted price from the day-ahead energy market. We also allow LSE to have a target for the total energy $E$ consumed over $[0, T]$ by the population of $N$ TCL customers, managed by the LSE. The choice of $E$ may be restricted by the parameters of the TCL population, an issue we address in Section III-B. To minimize its energy procurement cost, the LSE would like to schedule purchase of energy when $\widehat{\pi}(t)$ is low, and defer purchase when $\widehat{\pi}(t)$ is high, while satisfying the total energy budget ($E$), as well as maintaining the comfort constraints described below specified by each of the TCLs.

### C. Comfort Range Contracts

Each of the $N$ TCLs managed by an LSE, may have different comfort ranges $[L_{i0}, U_{i0}]$ with different tolerances $\Delta_i$, $i = 1, \ldots, N$. Let $\theta_i(t)$ be the indoor temperature of the $i^{\text{th}}$ home at time $t$. The LSE is obligated to maintain the indoor temperatures of its customer TCLs within their specified comfort ranges. That is, for each $i = 1, \ldots, N$, the LSE must ensure that $\theta_i(t) \in [L_{i0}, U_{i0}]$ for all $t \geq 0$. Such an agreement constitutes a contract between the LSE and an individual TCL.

An important part of this agreement is the flexibility of a load, captured by its range $2\Delta$. The LSE can utilize this flexibility to optimally time its purchase of power. The LSE's business model essentially consists of sharing part of the realized savings with the customers in terms of serving their needs for energy at low cost. Naturally, a customer with a greater flexibility $2\Delta$ is more valuable to the LSE and such customers can obtain better contracts from the LSE.

### D. Assumptions

For rest of this paper, we make the following assumptions.

- The ambient temperature forecast $\widehat{\theta}_a(t)$, and price forecast $\widehat{\pi}(t) > 0$, are continuous functions of time $t$.
- All TCLs are cooling, i.e., for all $t \in [0, T]$, we have $\widehat{\theta}_a(t) > \max_{i=1,\ldots,N} U_{i0}$.
- Each TCL in the population, when ON, draws the same thermal power $P$. Further, each TCL is assumed to have same load efficiency $\eta$.
- W.l.o.g., the initial indoor temperatures $\theta_{i0} := \theta_i(0) \in [L_{i0}, U_{i0}]$, for all $i = 1, \ldots, N$.

## III. Problem Formulation

Consider an LSE managing $N$ TCLs with thermal coefficients $\{\alpha_i, \beta_i\}_{i=1}^N$, initial conditions $\{(s_{i0}, \theta_{i0}, \sigma_{i0})\}_{i=1}^N$, and comfort tolerances $\{\Delta_i\}_{i=1}^N$. We now formulate the optimal power consumption design problem. We suppose that the LSE has available estimates [15], [16] of the parameters and initial conditions at the beginning of the time horizon.

### A. The Load Serving Entity's Objective

Denoting by $n_{\text{ON}}(t)$ the number of ON TCLs at time $t$, the aggregate electrical power drawn by the TCL population at time $t$ is $P_e n_{\text{ON}}(t) = \frac{P}{\eta}\sum_{i=1}^N u_i(t)$. We take the switching trajectories $\sigma_i(t)$ as decision variables $u_i(t) \in \{0,1\}$, and introduce an extended state vector $\boldsymbol{x}(t) := \left(\theta_1(t), \ldots, \theta_N(t), t, \int_0^t \sum_{i=1}^N u_i(\varsigma)\,\mathrm{d}\varsigma\right)^\top$ of size $(N+2)\times 1$. At time $t$, the components of $\boldsymbol{x}(t)$ are $x_i(t) := \theta_i(t)$ for $i = 1, \ldots, N$, $x_{N+1}(t) := t$, and $x_{N+2}(t) := \int_0^t \sum_{i=1}^N u_i(\varsigma)\,\mathrm{d}\varsigma$. Then, to minimize the procurement cost for total energy consumption over $[0, T]$, the LSE needs to:

$$\underset{u_1(t),\ldots,u_N(t)\in\{0,1\}^N}{\text{Minimize}} \frac{P}{\eta}\int_0^T \widehat{\pi}(t)\sum_{i=1}^N u_i(t)\,\mathrm{d}t, \tag{3}$$

subject to the constraints

**C1.** (Indoor temperature dynamics)

$$\left.\begin{aligned} \dot{x}_i(t) &= -\alpha_i(x_i(t) - \widehat{\theta}_a(t)) - \beta_i P u_i(t), \\ x_i(0) &= \theta_{i0}, \quad i = 1, \ldots, N, \end{aligned}\right\} \tag{4}$$

$$\dot{x}_{N+1}(t) = 1, \quad x_{N+1}(0) = 0, \quad x_{N+1}(T) = T, \tag{5}$$

**C2.** (Energy/isoperimetric constraint)

$$\dot{x}_{N+2}(t) = \sum_{i=1}^N u_i(t), x_{N+2}(0) = 0, x_{N+2}(T) = \frac{\eta E}{NP}, \tag{6}$$

**C3.** (Contractual comfort/state inequality constraint)

$$L_{i0} \le x_i(t) \le U_{i0}, \tag{7}$$

where $[L_{i0}, U_{i0}] := [s_{i0} - \Delta_i, s_{i0} + \Delta_i]$ for $i = 1, \ldots, N$. We notice that the constraints (4) and (7) are decoupled, while the cost function (3) and constraint (6) are coupled. Denoting the solution of the open loop deterministic optimal control problem (3)–(7) by $\{u_i^*(t)\}_{i=1}^N$, the optimal power consumption trajectory is given by $P_{\text{total}}^{\text{ref}}(t) = \frac{P}{\eta}\sum_{i=1}^N u_i^*(t)$.

*Remark 1:* The optimal control problem (3)–(7) is non-autonomous since there are explicit dependence on time in the cost function (via $\widehat{\pi}(t)$) and in the dynamics (via $\widehat{\theta}_a(t)$). This motivated us to include time $t$ as a component of $\boldsymbol{x}(t)$.

### B. Feasibility

Let $\tau := \frac{\eta E}{P}$, and notice that the constraint (6) imposes a necessary condition for feasibility,

$$0 \le \overline{\tau} := \frac{\tau}{NT} = \frac{\eta E}{NPT} = \frac{x_{N+2}(T)}{T} \le 1. \tag{8}$$

Given an ambient temperature forecast $\widehat{\theta}_a(t)$ and parameters of the TCL population, further restriction of $\overline{\tau}$ is needed to include the possibility of zero dynamics on (meaning the temperature trajectory chatters along) the boundaries $L_{i0}$ and $U_{i0}$. Such a restriction is of the form

$$0 \le \overline{\tau}_\ell \le \overline{\tau} \le \overline{\tau}_u \le 1, \tag{9}$$

where $\overline{\tau}_\ell := \frac{\tau_\ell}{NT} = \frac{\eta E_\ell}{NPT}$, and likewise for $\overline{\tau}_u = \frac{\eta E_u}{NPT}$. Here $E_\ell$ (resp. $E_u$) is the aggregate energy consumed if the entire population were to be maintained at their private upper (lower) setpoint boundaries, thus resulting in the lowest (highest) total energy consumption while respecting (7). In other words, $E_\ell = \frac{P}{\eta}\sum_{i=1}^N \int_0^T u_i(t)\,\mathrm{d}t$, where the zero dynamics controls are $u_i(t) = \frac{\alpha_i}{\beta_i P}\left(\widehat{\theta}_a(t) - U_{i0}\right)$, and hence

$$\overline{\tau}_\ell = \frac{1}{NP}\left(\sum_{i=1}^N \frac{\alpha_i}{\beta_i}\left(\langle\widehat{\theta}_a\rangle - U_{i0}\right)\right), \tag{10}$$

where $\langle\widehat{\theta}_a\rangle := \frac{1}{T}\int_0^T \widehat{\theta}_a(t)\,\mathrm{d}t$. Similar calculation yields

$$\overline{\tau}_u = \frac{1}{NP}\left(\sum_{i=1}^N \frac{\alpha_i}{\beta_i}\left(\langle\widehat{\theta}_a\rangle - L_{i0}\right)\right). \tag{11}$$

Thus, (9) characterizes the necessary and sufficient conditions for feasibility of the optimal control problem (3)–(7).

*Remark 2:* Notice that constraint **C2** expresses a total energy budget $\frac{P}{\eta}\int_0^T \sum_{i=1}^N u_i(t)\mathrm{d}t = E$. In the absence of **C2**, the optimal controls $\{u_i^*(t)\}_{i=1}^N$ that minimize (3) subject to **C1** and **C3**, satisfy $\frac{P}{\eta}\int_0^T \sum_{i=1}^N u_i^*(t)\mathrm{d}t = E_\ell$, where from (10), we have

$$E_\ell = \frac{T}{\eta}\left(\sum_{i=1}^N \frac{\alpha_i}{\beta_i}\left(\langle\widehat{\theta}_a\rangle - U_{i0}\right)\right). \tag{12}$$

*Remark 3:* Notice also that condition (9) is equivalent to the energy inequality $E_{\min} \le E_\ell \le E \le E_u \le E_{\max}$, where $E_{\min} := 0$, $E_{\max} := \frac{NPT}{\eta}$, $E_\ell$ is given by (12), and from (11) we have $E_u = \frac{1}{NP}(\sum_{i=1}^N \frac{\alpha_i}{\beta_i}(\langle\widehat{\theta}_a\rangle - L_{i0}))$. As a consequence, the feasible energy budget $E$ must belong to an interval $[E_\ell, E_u]$ with length $E_u - E_\ell = \frac{2T}{\eta}\sum_{i=1}^N \frac{\alpha_i}{\beta_i}\Delta_i$.

### C. Difficulty in Direct Numerical Simulation

A direct numerical approach converts the optimal control problem (3)–(7) to an optimization problem via time discretization. Such a "discretize-then-optimize" strategy leads to a mixed integer linear program (MILP), since $\theta_i(t) \in \mathbb{R}$ but $u_i(t) \in \{0,1\}$, for $i = 1, \ldots, N$. Typically, the day-ahead price forecast $\widehat{\pi}(t)$ is available as piecewise constant for each hour, and hence taking the Euler discretization for dynamics (4) with 1 minute time resolution results in an MILP over $24 \times 60 \times 2 \times N$ variables. In our experience, solving the MILP even for $N = 2$ homes for the day-ahead price, is computationally expensive (CPU runtime over 24 hours) in Gurobi [17]. On the other hand, a linear program (LP) relaxation of the MILP, resulting from the control convexification $u_i \in \{0,1\} \mapsto \widetilde{u}_i \in [0,1]$, has much faster runtime and was reported in our earlier work [18]. Furthermore, the optimal solution of the LP relaxation has the physical meaning of average ON duration over a discretization interval (see Fig. 2).

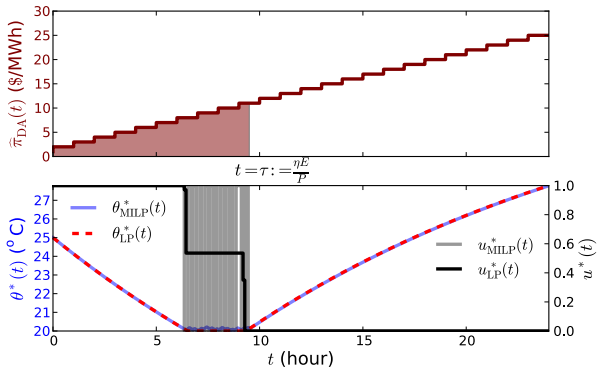


Fig. 2. Top: A monotone increasing day-ahead price forecast $\widehat{\pi}_{\rm DA}(t)$ that is piecewise constant for each hour, is shown with $\tau = \frac{\eta E}{P}$. Bottom: The corresponding solution of the optimal power consumption problem (3)–(7) via discretized MILP (from Gurobi) and LP (from MATLAB `linprog`) for $N = 1$ home with $[L_0, U_0] = [20°\text{C}, 30°\text{C}]$, and constant ambient forecast $\widehat{\theta}_a(t) = 32°\text{C}$. The parameter values used in this simulation are from Table 1, p. 1392 in [5].

However, the MILP equality constraint does not satisfy total unimodularity (see for example, Ch. 5 in [19]), and so the optimal solution of the LP relaxation is not the optimal solution of the MILP. In the following Sections IV and V, we solve the continuous time optimal control problem (3)–(7) using Pontryagin's maximum principle (PMP) [20], thereby obtaining qualitative insights into the optimal solution, which are otherwise difficult to gauge from the direct numerical solution of the discretized LP relaxation.

## IV. Solution of the Optimal Control Problem

For the optimal control problem (3)–(7), if we remove constraints **C2** and **C3**, then the optimal control is trivial: $u_i^*(t) = 0$ for all $i = 1, \ldots, N$, for all $t \in [0, T]$. In Section IV-A, we first discuss the non-trivial case of solving (3) subject to **C1** and **C2**, i.e., in the absence of the inequality constraints **C3**. This is followed by the solution for general case in Section IV-B, with all constraints **C1–C3** active.

### A. Solution with Constraint C3 Inactive

*Theorem 1:* Consider problem (3) with constraints **C1–C2**. The optimal controls are synchronizing, i.e., $u_1^*(t) = u_2^*(t) = \ldots = u_N^*(t)$ at each $t \in [0, T]$. There is a threshold price $\pi^*$, such that $u_i^* = 1(0)$ for all $i = 1, \ldots, N$, iff $\widehat{\pi}(t) < (\geq)\pi^*$. Specifically, let $\Phi_{\widehat{\pi}}(\widetilde{\pi}) := \int_0^T \mathbb{1}_{\{\widehat{\pi}(t) \leq \widetilde{\pi}\}}\, \mathrm{d}t$, $\pi^* := \inf\{\widetilde{\pi} \in \mathbb{R}^+ : \Phi_{\widehat{\pi}}(\widetilde{\pi}) = \frac{\tau}{N}\}$, $S := \left\{s \in [0, T] : \widehat{\pi}(s) < \pi^*\right\}$, and let $\boldsymbol{\lambda}$ be the costate vector corresponding to the state vector $\boldsymbol{x}$ in Section III-A. Then the optimal solution is

$$u_i^*(t) = \begin{cases} 1 & \forall t \in S \\ 0 & \text{otherwise,} \end{cases} \qquad \lambda_i^*(t) = 0 \; \forall i = 1, \ldots, N,$$

$$\lambda_{N+1}^*(t) = \begin{cases} \frac{P}{\eta} N \left(\pi^* - \widehat{\pi}(t)\right) & \forall t \in S, \\ 0 & \text{otherwise,} \end{cases} \quad \lambda_{N+2}^*(t) = -\frac{P}{\eta}\pi^*,$$

$$x_i^*(t) = e^{-\alpha_i t}\left(\theta_{i0} + \int_0^t e^{\alpha_i \varsigma}\left(\alpha_i \widehat{\theta}_a(\varsigma) - \beta_i P u_i^*(\varsigma)\right) \mathrm{d}\varsigma\right)$$

$$\forall i = 1, \ldots, N,\; x_{N+1}^*(t) = t,\; x_{N+2}^*(t) = \begin{cases} Nt & \forall t \in S, \\ 0 & \text{otherwise.} \end{cases}$$

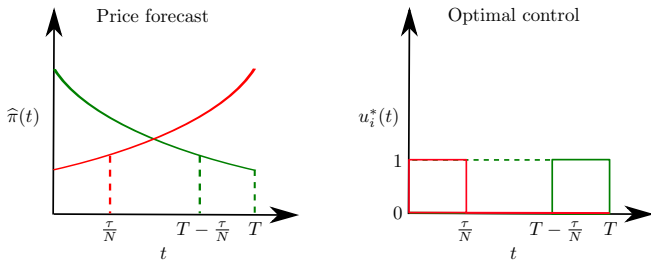


Fig. 3. Left: Strictly increasing (*red*) and decreasing (*green*) price forecasts $\widehat{\pi}(t)$, Right: the corresponding optimal control with constraint **C3** inactive is given by $u_i^*(t) = \mathbb{1}_S$, where $S = [0, \frac{\tau}{N}]$ for strictly increasing, and $S = [T - \frac{\tau}{N}, T]$ for strictly decreasing $\widehat{\pi}(t)$.

*Proof:* The Hamiltonian

$$H = \sum_{i=1}^{N} \Bigg[ u_i(t) \left( \frac{P}{\eta}\widehat{\pi}(t) - P\beta_i\lambda_i(t) + \lambda_{N+2}(t) \right) - \alpha_i\lambda_i(t)\left(x_i(t) - \widehat{\theta}_a(t)\right) \Bigg] + \lambda_{N+1}(t) \quad (13)$$

gives the first order optimality conditions

$$\dot{\lambda}_i(t) = -\frac{\partial H}{\partial x_i} = \alpha_i\lambda_i(t), \qquad i = 1, 2, \ldots, N, \quad (14)$$

$$\dot{\lambda}_{N+1}(t) = -\frac{\partial H}{\partial t} = -\frac{P}{\eta}\frac{\partial \widehat{\pi}}{\partial t}\sum_{i=1}^{N} u_i(t) - \frac{\partial \widehat{\theta}_a}{\partial t}\sum_{i=1}^{N}\alpha_i\lambda_i(t), \quad (15)$$

$$\dot{\lambda}_{N+2}(t) = -\frac{\partial H}{\partial x_{N+2}} = 0 \Rightarrow \lambda_{N+2} = \text{constant.} \quad (16)$$

The transversality condition yields $-\sum_{i=1}^{N}\lambda_i(T)\mathrm{d}x_i(T) - \lambda_{N+1}(T)\mathrm{d}x_{N+1}(T) - \lambda_{N+2}(T)\mathrm{d}x_{N+2}(T) + H(T)\mathrm{d}T = 0$. Since the terminal states $\theta_i(T)$ are free, $\mathrm{d}x_i(T) = \mathrm{d}\theta_i(T) \neq 0$ implying that $\lambda_i(T) = 0$, for all $i = 1, \ldots, N$. Since $T$ is fixed, $\mathrm{d}x_{N+1}(T) = \mathrm{d}T = 0$. Similarly, $\mathrm{d}x_{N+2}(T) = \frac{\mathrm{d}\tau}{N} = 0$. Combining $\lambda_i(T) = 0$ with (14) gives $\lambda_i(t) = 0$ for all $t$. Setting $\lambda_i(t) \equiv 0$ in (13), and invoking PMP yields the optimal controls as

$$\underset{(u_1(t), \ldots, u_N(t)) \in \{0,1\}^N}{\text{argmin}} \left(\frac{P}{\eta}\widehat{\pi}(t) + \lambda_{N+2}\right)\sum_{i=1}^{N} u_i(t). \quad (17)$$

Hence, if $\frac{P}{\eta}\widehat{\pi}(t) + \lambda_{N+2} > (<) 0$, then we need to minimize (maximize) $\sum_{i=1}^{N} u_i$ over $\{0, 1\}^N$, meaning that the *optimal controls are synchronized*.

We know $P, \eta, \widehat{\pi}(t) > 0 \; \forall\, t \in [0, T]$. Thus, if $\lambda_{N+2} \geq 0$, then $\frac{P}{\eta}\widehat{\pi}(t) + \lambda_{N+2} > 0$ implying $u_i^*(t) = 0 \; \forall i = 1, \ldots, N, \; \forall t \in [0, T]$ . This in turn leads to $\dot{x}_{N+2} = 0$ implying $x_{N+2}(t) = x_{N+2}(0) = 0 = x_{N+2}(T) = \frac{\tau}{N}$, which is impossible since $\tau \neq 0$ (given). Therefore, the constant $\lambda_{N+2} < 0$.

Notice that whether $\frac{P}{\eta}\widehat{\pi}(t) + \lambda_{N+2}$ is $> 0$ or $< 0$ depends on the magnitude of the constant $\lambda_{N+2} < 0$, as well as on the magnitude of $\widehat{\pi}(t) > 0$. Depending on the sign of the time-varying sum $\frac{P}{\eta}\widehat{\pi}(t) + \lambda_{N+2}$, the optimal control will switch between 0 and 1.

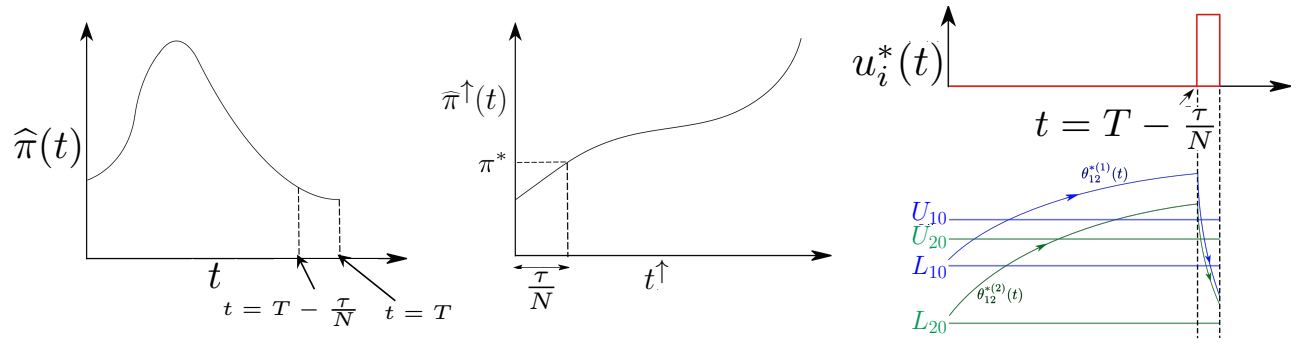


Fig. 4. Left: A non-monotone price forecast $\widehat{\pi}(t)$ with $S = [T - \frac{\tau}{N}, T]$ being the subset of times in $[0, T]$, with measure $\frac{\tau}{N}$, that corresponds to minimum price. Middle: $\widehat{\pi}^{\uparrow}(t)$ is the increasing rearrangement of the function $\widehat{\pi}(t)$, plotted against the corresponding re-arranged time $t^{\uparrow}$. Right: With constraint **C3** inactive, the optimal control $u_i^*(t)$ and optimal indoor temperature trajectories $\theta_{12}^{*(i)}(t)$ are shown for $i = 1, 2$ TCLs. The subscript $_{12}$ in $\theta_{12}^{*(i)}(t)$ denotes that constraints **C1** and **C2** are active.

Let us denote the optimal value of $\lambda_{N+2}$ as $\lambda^*_{N+2}$, and consider a set $S \subseteq [0, T]$ given by $S := \{s \in [0, T] : \widehat{\pi}(s) < -\frac{\eta}{P}\lambda^*_{N+2}\}$. Then, from PMP, $\forall\ i = 1, \ldots, N$, we can rewrite the optimal control as $u_i^*(t) = 1 \forall t \in S$, and $= 0$ otherwise. Thus, to determine $u_i^*(t)$, all that remains is to determine $\lambda^*_{N+2}$, or equivalently $-\frac{\eta}{P}\lambda^*_{N+2}$, where the latter can be interpreted as some threshold price $\pi^* > 0$. The choice of $\lambda_{N+2} < 0$, or equivalently $-\frac{\eta}{P}\lambda_{N+2} > 0$, is constrained by the terminal condition $x_{N+2}(T) = \frac{\tau}{N} \Leftrightarrow \int_0^T \sum_{i=1}^N u_i(t)\, \mathrm{d}t = \frac{\tau}{N} \overset{\text{PMP}}{\Longrightarrow} \int_0^T \sum_{i=1}^N \mathbb{1}_{\{\widehat{\pi}(t) < -\frac{\eta}{P}\lambda_{N+2}\}}\, \mathrm{d}t = \frac{\tau}{N}$, and hence the feasible choices of $-\frac{\eta}{P}\lambda_{N+2}$ comprise the set $\{-\frac{\eta}{P}\lambda_{N+2} \in \mathbb{R}^+ : \int_0^T \mathbb{1}_{\{\widehat{\pi}(t) < -\frac{\eta}{P}\lambda_{N+2}\}}\, \mathrm{d}t = \frac{\tau}{N}\}$. The optimal $\lambda^*_{N+2}$, that minimizes the "cost-to-go" $\frac{P}{\eta}\int_0^T \widehat{\pi}(t) \sum_{i=1}^N \mathbb{1}_{\{\widehat{\pi}(t) < -\frac{\eta}{P}\lambda_{N+2}\}} \mathrm{d}t$, is given by $-\frac{\eta}{P}\lambda^*_{N+2} = \inf\big\{ -\frac{\eta}{P}\lambda_{N+2} \in \mathbb{R}^+ : \int_0^T \mathbb{1}_{\{\widehat{\pi}(t) < -\frac{\eta}{P}\lambda_{N+2}\}}\, \mathrm{d}t = \frac{\tau}{N}\big\}$.

To determine $\lambda^*_{N+1}(t)$, combining (15) with $\lambda_i(t) = 0$ results in $\dot{\lambda}_{N+1} = -\frac{P}{\eta} N \mathbb{1}_{\{\widehat{\pi}(t) < -\frac{\eta}{P}\lambda^*_{N+2}\}} \frac{\partial \widehat{\pi}}{\partial t}$. Thus, $\lambda_{N+1}|_{u_i^*(t)=0} = H|_{u_i^*(t)=0} =$ constant, which we enforce to be zero. On the other hand, $\lambda_{N+1}|_{u_i^*(t)=1} = -\frac{P}{\eta} N \widehat{\pi}(t) + k$, where the integration constant $k$ needs to be determined. Since $H|_{u_i^*(t)=1} = N\left(\frac{P}{\eta}\widehat{\pi}(t) + \lambda^*_{N+2}\right) + \lambda_{N+1}|_{u_i^*(t)=1} = N\lambda^*_{N+2} + k =$ constant, which, as before, we enforce to be zero, we obtain $k = -N\lambda^*_{N+2} \Rightarrow \lambda_{N+1}|_{u_i^*(t)=1} = -\frac{P}{\eta} N \widehat{\pi}(t) - N\lambda^*_{N+2} = \frac{P}{\eta} N\left(\pi^* - \widehat{\pi}(t)\right) > 0$, as $\pi^* > \widehat{\pi}(t)$ $\forall t \in S$.

To derive $x_i^*(t)$ for all $i = 1, \ldots, N$, we simply substitute the optimal control $u_i^*(t)$ and then integrate the resulting first-order linear non-homogeneous ODE (4) using the method of integrating factor, to get the desired expression. ■

*Remark 4:* Monotone rearrangement of $\widehat{\pi}(t)$: The main insight behind the optimal control derived in Theorem 1 can be obtained by looking at strictly monotone price forecasts, as shown in Fig. 3. In these cases, it is intuitive that the optimal ON periods of the TCLs lie at either end of the interval $[0, T]$. Theorem 1 asserts that the same insight can be extended to non-monotone $\widehat{\pi}(t)$, by first computing its monotone rearrangement (p. 276, Ch. 10 in [21]) $\widehat{\pi}^{\uparrow}(t)$, and then computing the threshold $\pi^*$ and the ON time set $S$ from this monotone rearrangement as a function of $\frac{\tau}{N}$, as illustrated in Fig. 4.

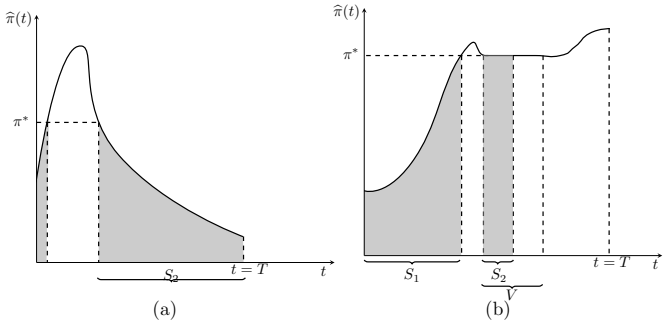


Fig. 5. (a) For this non-monotone price forecast, the set $S = S_1 \cup S_2$ is unique, where $|S| = \frac{\tau}{N}$, and hence $u_i^*(t)$ is unique too. (b) Here also $S = S_1 \cup S_2$ such that $|S| = \frac{\tau}{N}$, however, $\frac{\tau}{N}$ and hence the threshold $\pi^*$ are such that the set $S_2 \subset V$, where $V$ is the total interval of constancy. Thus, subsets of $S_2$ can be interchanged with equi-measure subsets of $V \backslash S_2$ without affecting the cost. Therefore, the set $S$ and optimal control $u_i^*(t)$ are not unique in this case. Since these sets are continuous, the number of such interchanges, and hence the number of optimal controls, is uncountable.

*Remark 5:* Non-uniqueness of optimal control: From Theorem 1, the synchronized optimal control $\{u_i^*(t)\}_{i=1}^N$, is unique iff the set $S$ is unique, where $S$ is the pre-image of $\pi^*$. Notice that although $\pi^*$ is unique for any continuous $\widehat{\pi}(t)$, uniqueness of $S$ depends on whether there exist time intervals of constancy in price forecast $\widehat{\pi}(t)$. For example, in Fig. 4, there is no such interval of constancy, and hence the pre-image set $S$, and the optimal control $u_i^*(t)$, are unique. This remains true even when $\frac{\tau}{N}$ is large (see Fig. 5(a)). Non-uniqueness, however, can arise if there exist an interval of constancy $V$, and $\frac{\tau}{N}$ is large enough that $S$ contains at least a subset of $V$ (see Fig. 5(b)). The uncountable number of non-unique solutions arising from such a situation can be resolved by fixing the convention of choosing the optimal control with minimum number of switchings.

### *B. Solution with Zero Amplitude Chattering*

Now we solve (3)–(7) subject to constraints (**C1**)–(**C3**), under the assumption that the indoor temperature trajectories $\theta_i(t)$ can slide along the boundaries $L_{i0}$ and $U_{i0}$, which can be thought of as the limit of small amplitude chattering. We

assume that sliding along $L_{i0}$ holds the ON mode, while the same along $U_{i0}$ holds the OFF mode. Our objective is to obtain qualitative insight into the solution structure under these simplifying assumptions. In Section V, we consider the practical case of finite amplitude chattering.

To describe the optimal solution, we next define the two-sided Skorokhod map [22], [23], which generalizes the one-sided version originally introduced by Skorokhod [24].

*Definition 1:* Two-sided Skorokhod Map:
Given $0 < L < U < \infty$, and scalar trajectory $y(\cdot) \in \mathbb{D}(-\infty, \infty)$, the two-sided Skorokhod map $\Psi_{L,U} : \mathbb{D}(-\infty, \infty) \mapsto \mathbb{D}[L, U]$ is defined as $z(t) = \Psi_{L,U}(y(t)) := \Lambda_{L,U} \circ \Psi_{L,\infty}(y(t))$, where $\Lambda_{L,U}(\phi)(t) := \phi(t) - \sup_{0 \le s \le t} \left( [\phi(s) - U]^+ \wedge \inf_{s \le r \le t} (\phi(r) - L) \right)$, and $\Psi_{L,\infty}(y(t)) := y(t) + \sup_{0 \le s \le t} [L - y(s)]^+$.

*Theorem 2:* Consider problem (3) with constraints **C1**–**C3**. The optimal controls are synchronizing, and, as in Theorem 1, based on a price forecast threshold $\pi^*$, switch between 0 and 1. Assuming zero amplitude chattering to be feasible, the open loop optimal controls $u_i^*(t)$ are identical to those in Theorem 1. For $i = 1, \ldots, N$, the optimal states $x_i^*(t)$ are the two-sided Skorokhod maps parameterized by individual comfort ranges $[L_{i0}, U_{i0}]$, acting on respective optimal states from Theorem 1, i.e., $\theta_{123}^{*(i)}(t) = \Psi_{L_{i0},U_{i0}}\left(\theta_{12}^{*(i)}(t)\right)$, where $\theta_{123}^{*(i)}(t)$ is the optimal indoor temperature trajectory when constraints **C1**–**C3** are active, and $\theta_{12}^{*(i)}(t)$ is the same when constraints **C1**–**C2** are active, for the $i^{\text{th}}$ TCL.

*Proof:* From the necessary conditions for optimality under state inequality constraints [25], [26], it can be directly verified that the $\pi^*$ is as in Theorem 1. Hence the monotone rearrangement argument applies as before, and $u_i^*(t)$ are synchronized as function of time. However, the optimal states have different hitting times to the respective boundaries $L_{i0}$ and $U_{i0}$. For brevity, we provide below a simple graphical argument for the optimal states for strictly monotone (w.l.o.g. decreasing) $\widehat{\pi}(t)$. The non-monotone $\widehat{\pi}(t)$ can be dealt via the monotone rearrangement, and the non-uniqueness due to constancy can be dealt with by adopting a minimum switching convention, as earlier.

By the argument above, consider strictly decreasing $\widehat{\pi}(t)$ as in Fig. 3 left, green curve, and fix the $i^{\text{th}}$ home with initial indoor temperature $\theta_{i0}$, and comfort boundaries $L_{i0}$ and $U_{i0}$. At time $t = 0^+$, the trajectory $\theta_i(t)$ can move either exponentially upward or downward. For $t \in [0, T]$, let us call the set of all feasible trajectories $\theta_i(t) \in [L_{i0}, U_{i0}]$ for which $u_i(0^+) = 0$, as the "initially up-going family". Similarly, define "initially down-going family" for $u_i(0^+) = 1$. Our proof consists of the following two steps.

Step 1: Finding the optimal indoor temperature trajectory among the "initially up-going family": We notice that among the "initially up-going family", it is optimal to hit $U_{i0}$, since otherwise turning the TCL ON before hitting $U_{i0}$ strictly increases the cost, as $\widehat{\pi}(t)$ is strictly decreasing. Similarly, starting from the time at which $U_{i0}$ is hit, it is then optimal to hold till $T - \frac{\tau}{N}$ as sliding along $U_{i0}$, as per assumption, does not contribute to the cost. For $t \in [T - \frac{\tau}{N}, T]$, we notice that we must keep $u_i(t) = 1$ to respect the energy constraint. Further, notice that any de-synchronization among TCLs increase cost. Thus, the optimal temperature trajectory among the "initially up-going family" looks like those shown in Fig. 6 bottom right. From Definition 1, we find that the optimal indoor temperature trajectory among the "initially up-going family" is $\Psi_{L_{i0},U_{i0}}\left(\theta_{12}^{*(i)}(t)\right)$.

Step 2: Showing that any trajectory from the "initially down-going family" has cost strictly larger than the same for the optimal trajectory in Step 1: This can be easily verified by comparing the optimal from Step 1, with any trajectory from the "initially down-going family" using that $\widehat{\pi}(t)$ is strictly decreasing.

Combining the above two steps, we conclude that for $\widehat{\pi}(t)$ strictly decreasing, the optimal indoor temperature trajectory found in Step 1 is the optimal among all feasible indoor temperature trajectories. Similar argument applies to $\widehat{\pi}(t)$ strictly increasing, and to monotone rearranged version $\widehat{\pi}^{\uparrow}(t)$ in case $\widehat{\pi}(t)$ is non-monotone. We eschew the details and illustrate an example in Fig. 6 to help the readers follow our main argument. ■

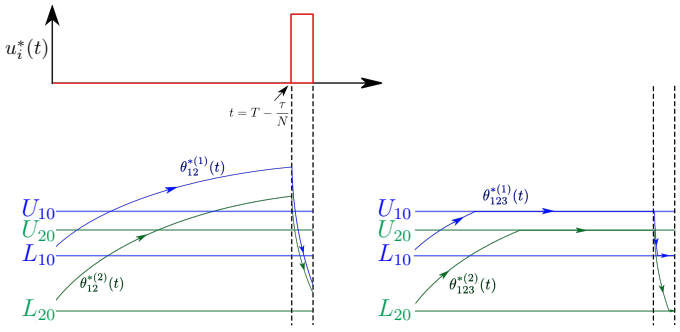


Fig. 6. For the non-monotone price forecast $\widehat{\pi}(t)$ same as in Fig. 4, the optimal controls $u_i^*(t)$ (top left) with constraints **C1**–**C3**, are same as those shown in Fig. 4. However, the optimal indoor temperatures $\theta_{123}^{*(i)}(t)$ (right bottom) are different from $\theta_{12}^{*(i)}(t)$ (left bottom, same as in Fig. 4), for $i = 1, 2$ TCLs. The subscript $_{123}$ in $\theta_{123}^{*(i)}(t)$ denotes that constraints **C1**–**C3** are active.

## V. Implementable Solution with A Specified Minimum Switching Period

Since physical thermostats have a minimum chattering amplitude, or equivalently minimum ON-OFF time period $T_m > 0$, it is important to find an algorithm that explicitly accounts this device limit into control design. Given this parameter $T_m$, the following Theorem gives an *exact* algorithm to compute the binary optimal control via convexification.

*Theorem 3:* For $i = 1, \ldots, N$, consider the control convexification $u_i(t) \in \{0, 1\} \mapsto v_i(t) \in [0, 1]$, and let $v_i^*(t) \in [0, 1]$ be the optimal convexified control corresponding to the non-convex optimal control problem (3)–(7) with $N$ TCLs having thermal coefficients $\{\alpha_i, \beta_i\}_{i=1}^N$. Let $\vartheta_i^*(t)$ (resp. $\theta_i^*(t)$) be the indoor temperature trajectory realized by the optimal control $v_i^*(t)$ (resp. $u_i^*(t)$). Then, the following algorithm recovers the optimal control $u_i^*(t) \in \{0, 1\}$ from

$v_i^*(t) \in [0,1]$, while guaranteeing that the indoor temperatures trajectories $\vartheta_i^*(t)$ and $\theta_i^*(t)$ coincide at the end of each minimum allowable time period of length $T_m$.

**Algorithm 1** Recovering $u_i^*(t) \in \{0,1\}$ from $v_i^*(t) \in [0,1]$

**if** $v_i^*(t) = 0$ OR $1$ **then**
  $u_i^*(t) = v_i^*(t)$
**else**
  **if** $\vartheta_i^*(t)$ is at upper boundary **then**
    $$u_i^*(t) = \begin{cases} 1 & \forall\, t \in [(j-1)T_m, (j-1)T_m + \overline{\gamma}_i) \\ 0 & \forall\, t \in [(j-1)T_m + \overline{\gamma}_i, jT_m) \end{cases}$$
    where $j = 1, \ldots, \lceil \frac{\text{spt}(v_i^*(t))}{T_m} \rceil$, $t \in [0, T]$
  **else** $\vartheta_i^*(t)$ is at lower boundary
    $$u_i^*(t) = \begin{cases} 0 & \forall\, t \in [(j-1)T_m, jT_m - \underline{\gamma}_i) \\ 1 & \forall\, t \in [jT_m - \underline{\gamma}_i, jT_m) \end{cases}$$
    where $j = 1, \ldots, \lceil \frac{\text{spt}(v_i^*(t))}{T_m} \rceil$, $t \in [0, T]$
  **end if**
**end if**

In Algorithm 1, $\{(\overline{\gamma}_i, \underline{\gamma}_i)\}_{i=1}^N$ are time duration pairs such that the binary optimal trajectory $u_i^*(t)$ consists of two duty cycles: $\frac{\overline{\gamma}_i}{T_m}$ and $\frac{\underline{\gamma}_i}{T_m}$, where

$$\overline{\gamma}_i = \frac{1}{\alpha_i} \log \left( 1 + \alpha_i \int_0^{T_m} e^{\alpha_i s} v_i^*(s)\, \mathrm{d}s \right), \quad (18)$$

$$\underline{\gamma}_i = \frac{1}{\alpha_i} \log \left( \frac{1}{1 - \alpha_i e^{-\alpha_i T_m} \int_0^{T_m} e^{\alpha_i s} v_i^*(s)\, \mathrm{d}s} \right). \quad (19)$$

*Proof:* Since $v_i^*(t)$ is binary iff the respective upper and lower comfort boundaries are not hit, hence $u_i^*(t) = v_i^*(t)$ when $v_i^*(t) = 0$ or 1. We know that $v_i^*(t) \in (0,1)$ iff $\vartheta^*(t)$ is at either upper or lower boundary. Clearly, at the upper (lower) boundary, such cycles should begin with an ON (OFF) segment, and end with an OFF (ON) segment. Matching indoor temperature values at each end of these switching period means $\vartheta_i^*(T_m) = \theta_i^*(T_m)$, which gives

$$\int_0^{T_m} e^{\alpha_i s} v_i^*(s)\, \mathrm{d}s = \int_0^{T_m} e^{\alpha_i s} u_i^*(s)\, \mathrm{d}s. \quad (20)$$

At upper boundary, RHS of (20) equals $\int_0^{\overline{\gamma}_i} e^{\alpha_i s}\, \mathrm{d}s$, which solved for $\overline{\gamma}_i$ yields (18). At lower boundary, RHS of (20) equals $\int_{T_m - \underline{\gamma}_i}^{T_m} e^{\alpha_i s}\, \mathrm{d}s$, which solved for $\underline{\gamma}_i$ yields (19). ■

## VI. Numerical Simulation

To illustrate how the LSE can use the results derived so far for the purpose of demand response, we now provide a numerical example where the LSE computes the day-ahead minimum cost energy procurement for its $N = 500$ customers' TCLs based on ERCOT day-head price forecast $(\widehat{\pi}(t))$ data [27] for Houston on August 10, 2015, and the ambient temperature forecast $(\widehat{\theta}_a(t))$ data for the same day available from a weather station in Houston, Texas. These forecast data and the real-time ambient temperature $(\theta_a(t))$ data on August 11, 2015, are shown in Fig. 7.

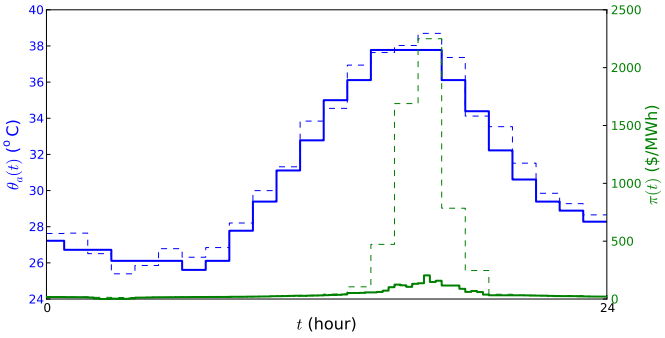


Fig. 7. The day-ahead ambient temperature forecast $\widehat{\theta}_a(t)$ (*dashed blue*), real-time ambient temperature $\theta_a(t)$ (*solid blue*), ERCOT day-ahead price $\widehat{\pi}(t)$ (*dashed green*), and ERCOT real-time price $\pi(t)$ (*solid green, not used for computation in this paper*) data for Aug. 11, 2015 in Houston.

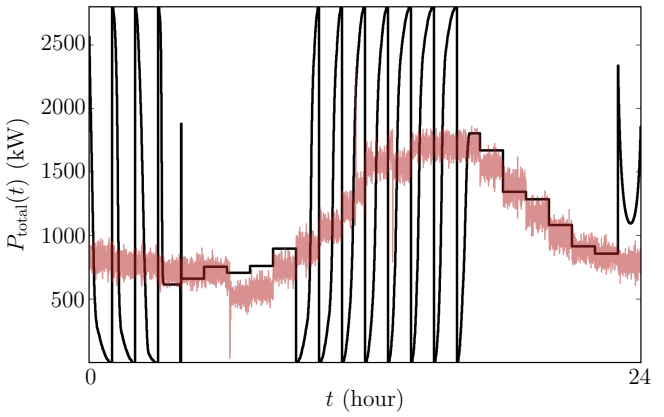


Fig. 8. The *black* curve shown above is the optimal power consumption trajectory $P_{\text{total}}^{\text{pref}}(t) = P_e \sum_{i=1}^N u_i^*(t)$ computed by solving the optimal control problem (3)–(7), via Algorithm 1 with $T_m = 1.5$ minutes. The *brick* colored curve is the real-time controlled aggregate consumption $P_{\text{total}}(t)$ corresponding to control gain tuple $(k_p, k_i, k_d) = (10^{-4}, 10^{-6}, 10^{-4})$ used to move the thermostatic boundaries (see Section III.1 in [28] for details). The LSE can invoke demand response by controlling the setpoints of the TCL population in such a way that their real-time aggregate consumption $P_{\text{total}}(t)$ track the reference aggregate consumption $P_{\text{total}}^{\text{pref}}(t)$. The tracking error between the two curves depend on the forecasted versus real-time ambient temperature mismatch, as well as on the thermal inertia of the TCLs in the population.

With the initial conditions and parameters of the heterogeneous TCL population as in Section V-A in [28], $\overline{\tau} = \frac{1}{3}$ (which was verified to be feasible using (9)), comfort tolerances $\{\Delta_i\}_{i=1}^N$ sampled randomly from a uniform distribution over $[0.1°\text{C}, 1.1°\text{C}]$, and for $\widehat{\pi}(t)$ and $\widehat{\theta}_a(t)$ as in Fig. 7, the LSE solves the optimal control problem (3)–(7) by first convexifying the controls $u_i(t) \in \{0,1\} \mapsto v_i(t) \in [0,1]$ for $i = 1, \ldots, N$, and then recovering the optimal controls $\{u_i^*\}_{i=1}^N$ using Theorem 3. For this computation, we used 1 minute time-step for Euler discretization of dynamics (4), and solved the resulting LP with 1 million 440 thousand decision variables (see Section III-C) using MATLAB `linprog`, followed by Algorithm 1 with $T_m = 1.5$ minutes. The resulting optimal power consumption trajectory $P_{\text{total}}^{\text{pref}}(t) = P_e \sum_{i=1}^N u_i^*(t)$ is shown as the black curve in Fig. 8. The brick colored curve in Fig. 8 correspond to the actual aggregate consumption for the TCL population with same $T_m$, and real-time ambient temperature $\theta_a(t)$ as in the solid

blue curve in Fig. 7, for a PID velocity control gain tuple $(k_p, k_i, k_d)$ used to control the setpoint boundaries as part of a mixed centralized-decentralized control. We refer the readers to Section III.1 in [28] for details on the real-time setpoint control. The purpose of Fig. 8 is to highlight how the solution of the open-loop optimal control problem (3)–(7) can be used by the LSE as a reference aggregate consumption to be tracked in real-time, to elicit demand response.

## VII. Concluding Remarks

In this paper, we addressed how an aggregator or load serving entity can design an optimal aggregate power consumption trajectory for a population of thermostatically controlled loads. We formulated this operational planning problem as a deterministic optimal control problem in terms of the day-ahead price forecast, ambient temperature forecast, and an energy budget available from the load forecast. We discuss why a direct numerical approach to solve the problem is computationally hard. Finally, we use tools from optimal control theory to gain analytic insights for the solution of the problem of designing optimal power consumption while respecting individual comfort range constraints. A numerical example is worked out to illustrate how an LSE can use the optimal aggregate power consumption trajectory computed offline, as a reference signal to be tracked in real-time by its customers' TCL population for the purpose of demand response.

## References


[1] U.S. Department of Energy, Benefits of Demand Response in Electricity Markets and Recommendations for Achieving Them. *A Report to the United States Congress Pursuant to Section 1252 of the Energy Policy Act of 2005*, Feb. 2006.

[2] D.S. Callaway, and I.A. Hiskens, "Achieving Controllability of Electric Loads". *Proceedings of the IEEE*, Vol. 99, No. 1, pp. 184–199, 2011.

[3] C.-Y. Chong, and A.S. Debs, "Statistical Synthesis of Power System Functional Load Models". *Proceedings of the 18th IEEE Conference on Decision and Control including the Symposium on Adaptive Processes*, No. 18, pp. 264–269, 1979.

[4] R. Malhamé, and C.-Y. Chong, "Electric Load Model Synthesis by Diffusion Approximation of a High-Order Hybrid-State Stochastic System". *IEEE Transactions on Automatic Control*, Vol. 30, No. 9, pp. 854–860, 1985.

[5] D.S. Callaway, "Tapping the Energy Storage Potential in Electric Loads to Deliver Load Following and Regulation, with Application to Wind Energy". *Energy Conversion and Management*, Vol. 50, No. 5, pp. 1389–1400, 2009.

[6] S. Bashash, and H.K. Fathy, "Modeling and Control Insights into Demand-side Energy Management through Setpoint Control of Thermostatic Loads". *Proceedings of the American Control Conference*, pp. 4546–4553, 2011.

[7] S. Kundu, N. Sinitsyn, S. Backhaus, and I. Hiskens, "Modeling and Control of Thermostatically Controlled Loads". *Proceedings of the 17th Power Systems Computation Conference*, Stockholm, Sweden, 2011.

[8] J.L. Mathieu, S. Koch, and D.S. Callaway, "State Estimation and Control of Electric Loads to Manage Real-time Energy Imbalance". *IEEE Transactions on Power Systems*, Vol. 28, No. 1, pp. 430–440, 2013.

[9] W. Zhang, J. Lian, C.-Y. Chang, and K. Kalsi, "Aggregate Modeling and Control of Air Conditioning Loads for Demand Response". *IEEE Transactions on Power Systems*, Vol. 28, No. 4, pp. 4655–4664, 2013.

[10] L.C. Totu, and R. Wisniewski, "Demand Response of Thermostatic Loads by Optimized Switching-Fraction Broadcast". *IFAC World Congress*, pp. 9956–9961, 2014.

[11] A. Ghaffari, S. Moura, and M. Krstić, "Analytical Modeling and Integral Control of Heterogeneous Thermostatically Controlled Load Populations". *ASME 2014 Dynamic Systems and Control Conference*, 2014.

[12] S. Meyn, P. Barooah, A. Bušić, Y. Chen, and J. Ehren, "Ancillary Service to the Grid using Intelligent Deferrable Loads". *IEEE Transactions on Automatic Control*, Vol. 60, No. 11, pp. 2847–2862, 2015.

[13] S. Grammatico, B. Gentile, F. Parise, and J. Lygeros, "A Mean Field Control Approach for Demand Side Management of Large Populations of Thermostatically Controlled Loads". *Proceedings of the European Control Conference*, pp. 3548–3553, 2015.

[14] D. Paccagnan, M. Kamgarpour, and J. Lygeros, "On the Range of Feasible Power Trajectories for A Population of Thermostatically Controlled Loads". *Proceedings of the 2015 IEEE 54th Annual Conference on Decision and Control (CDC)*, pp. 5883–5888, 2015.

[15] S. Moura, J. Bendtsen, and V. Ruiz, "Observer Design for Boundary Coupled PDEs: Application to Thermostatically Controlled Loads in Smart Grids". *Proceedings of the 52nd IEEE Conference on Decision and Control*, pp. 6286–6291, 2013.

[16] S. Moura, J. Bendtsen, and V. Ruiz, "Parameter Identification of Aggregated Thermostatically Controlled Loads for Smart Grids using PDE Techniques". *International Journal of Control*, pp. 1373–1386, Vol. 87, No. 7, 2014.

[17] Gurobi Optimization, Inc., "Gurobi Optimizer Reference Manual". `http://www.gurobi.com`, 2015.

[18] A. Halder, X. Geng, G. Sharma, L. Xie, and P.R. Kumar, "A Control System Framework for Privacy Preserving Demand Response of Thermal Inertial Loads". *Proceedings of the IEEE International Conference on Smart Grid Communications*, pp. 181–186, 2015.

[19] A. Schrijver, *Combinatorial Optimization: Polyhedra and Efficiency*. Vol. 24, Springer Science & Business Media, 2002.

[20] L.S. Pontryagin, V.G. Boltyanskii, R.V. Gamkrelidze, and E.F. Mishchenko, *The Mathematical Theory of Optimal Processes*. 1st ed. New York, NY: Wiley, 1962.

[21] G.H. Hardy, J.E. Littlewood, and G. Pólya, *Inequalities*. 2nd ed. Cambridge University Press, 1952.

[22] L. Kruk, J. Lehoczky, K. Ramanan, and S. Shreve, "An Explicit Formula for the Skorokhod Map on $[0, a]$". *The Annals of Probability*, Vol. 35, No. 5, pp. 1740–1768, 2007.

[23] L. Kruk, J. Lehoczky, K. Ramanan, and S. Shreve, "Double Skorokhod Map and Reneging Real-time Queues". *Markov Processes and Related Topics: A Festschrift for Thomas G. Kurtz*, Institute of Mathematical Statistics, pp. 169–193, 2008.

[24] A.V. Skorokhod, "Stochastic Equations for Diffusion Processes in a Bounded Region". *Theory of Probability & Its Applications*, Vol. 6, No. 3, pp. 264–274, 1961.

[25] A.E. Bryson, W.F. Denham, and S.E. Dreyfus, "Optimal Programming Problems with Inequality Constraints". *AIAA journal*, Vol. 1, No. 11, pp. 2544–2550, 1963.

[26] R.B. Vinter, *Optimal Control*, Birkhäuser, Boston, 2000.

[27] `http://tinyurl.com/z3gmvt6`, accessed on Sep. 17, 2016.

[28] A. Halder, X. Geng, P.R. Kumar, and L. Xie, "Architecture and Algorithms for Privacy Preserving Thermal Inertial Load Management by A Load Serving Entity". *arXiv manuscript:* `http://arxiv.org/abs/1606.09564`, 2016.